Spectrochimica Acta Part A: Molecular and Biomolecular Spectroscopy 227 (2020) 117748

Contents lists available at ScienceDirect

Spectrochimica Acta Part A: Molecular and Biomolecular Spectroscopy

journal homepage: www.elsevier.com/locate/saa

Spectrophotometric ellipsometry based Tat-protein RNA-aptasensor for HIV-1 diagnosis

Mustafa Oguzhan Caglayan [a,b], Zafer Üstündağ [c,*]

[a] Bilecik Şeyh Edebali University, Faculty of Eng., Department of Bioengineering, 11210 Bilecik, Turkey
[b] Cumhuriyet University, Nanotechnology Department, 58140 Sivas, Turkey
[c] Dumlupınar University, Faculty of Arts and Science, Chemistry Department, 43100 Kütahya, Turkey

ARTICLE INFO

Article history:
Received 24 September 2019
Received in revised form 31 October 2019
Accepted 1 November 2019
Available online 5 November 2019

Keywords:
HIV
Trans- activator of transcription
RNA- aptamer
Aptasensors
Spectroscopic ellipsometry
Surface plasmon resonance

ABSTRACT

Rapid and reliable diagnosis of Human Immunodeficiency Virus (HIV) Type I that causes autoimmune deficiency syndrome (AIDS) is still important today. In this study, the HIV-I Tat (trans-activator of transcription) protein-specific RNA-aptamer (antiTat) and spectroscopic ellipsometer were preferred to increase specificity and sensitivity in the diagnosis. The ellipsometry is a well-known characterization tool for the ultra-thin films, where polarization state changes show surface deposition in terms of the ellipsometric angles, psi (Ψ) and delta (Δ). Here, we reported the HIV-Tat protein detection performance of antiTat aptamers both for the spectroscopic ellipsometry (SE) and for the surface plasmon resonance enhanced total internal reflection ellipsometry (SPReTIRE), first time. Detection limits for antiTat aptamers with various configurations were in the range of nM-pM protein in the buffer solution. For instance, SPRe-TIRE configuration revealed a detection limit of 1 pM (or about 1.5 pg/mL) for HIV-Tat protein in the range of 1.0–500 nM.

1. Introduction

Epidemiological data on autoimmune deficiency syndrome (AIDS) indicate that rapid and sensitive diagnostic techniques should be developed to detect the virus as soon as possible following the infection [1]. Moreover, treatments using antiviral agents require a diagnosis of human immunodeficiency virus type I (HIV Type 1) as early as possible [2]. Antibody-based assays are available for the identification of HIV. Serological tests such as enzyme-linked immunosorbent assays (ELISA), particle adhesion assays, nucleic acid amplification by polymerase chain reaction (PCR) and Western blot (WB) assays are routine HIV antibody detection methods used to diagnose and validate HIV infection [3,4]. Commercial ultrasensitive HIV-gp24 glycoprotein capsid antigen-specific ELISAs often use an amplification technique, allow the detection of low antigen concentrations in the range of 0.2–10 pg/mL [5–8]. However, they require specific reagents and sophisticated, large and costly equipment and detailed sample preparation stages which are often necessary for optimal results [9–11]. Therefore, it is important to develop alternative detection techniques with comparable sensitivity and molecular specificity. Also these techniques should be applied as a simple assay format. To this end, various studies have been carried out on the development of alternative HIV diagnostic methods. A comprehensive review article on point-of-care (POC) technologies capable of providing early diagnosis of HIV has been published [12]. A plasmonic nanoprobe for HIV-1 GAG gene (126 bp), consisting of a stem-loop DNA molecule labeled with the Raman-tag and a metal nanoparticle has been proposed [13]. Homogeneous genotyping analyses based on various fluorescence resonance energy transfer techniques that employ hybridization techniques with PCR products has also been reported in the literature [14,15].

There are limited numbers of studies dealing with the aptamer applications, in the literature. Aptamers are oligonucleotides that can bind target molecules such as drugs, proteins, or even small inorganics, with high affinity and specificity [16,17]. Aptamers are obtained by an in vitro selection method called SELEX (systematic evolution of ligands by exponential enrichment) which was reported in 1990 [18,19]. This method allows the identification of unique oligonucleotide sequence, which selectively binds to a specific target, from a random library [20]. Aptamers have got comparable or even better affinity than some monoclonal antibodies, since their dissociation coefficients typically in the range of μM to pM [21], therefore they are defined as synthetic antibodies. Moreover, their selectivity to their targets can be 10,000-fold more than the interfering molecule [21]. There are a large number of different aptamers have been reported for various targets such as organic dyes,

* Corresponding author.
E-mail address: zafer.ustundag@dpu.edu.tr (Z. Üstündağ).

https://doi.org/10.1016/j.saa.2019.117748
1386-1425/

amino acids, antibiotics, peptides, proteins, vitamins and viruses [22–25].

HIV-Tat protein is a protein consisting of 101 amino acids and controls the first stages of the HIV-1 replication cycle [26–28]. There are very limited numbers of papers involving on the determination of this protein. Published studies have generally been performed with peptides derived from HIV-Tat [29,30]. HIV-Tat protein binds to HIV-1 RNA, which shows a natural affinity for the TAR (Trans-Activated Response) element of the virus [27]. An RNA-aptamer specific for Tat-protein has been reported in the literature [31]. This aptamer has a similar structure to the TAR and shows a 130-fold greater affinity for HIV-Tat protein compared to TAR [32].

Ellipsometry and spectroscopic ellipsometry (SE) methods precisely determine the optical properties of ultra-thin films such as thickness, refraction index by examining the variation between the states of polarization of light which reflected from a surface and passing through the thin film. Ellipsometry determines the complex reflectance ratio of p- and s-polarized light which are defined as the function of two ellipsometric angles, Δ and Ψ, in relation with each other as in Eq. (1) [33].

$$\rho = \frac{r_p}{r_s} = \tan\Psi . e^{i\Delta} \tag{1}$$

In the SE method, molecular deposition in case of aptamer-target interaction changes both thickness and optical properties of deposited layer film on the substrate (Fig. 1a). Among the optical properties, Δ is sensitive to this deposition.

Surface plasmon resonance (SPR) aided total internal reflection ellipsometry (TIRE), on the other hand, is a technique in which molecular deposition can be observed very precisely due to the infinite slope change of Δ at SPR conditions. In this method, SPR conditions are met using a flow cell configuration assembled as attenuated total internal reflection setup (Fig. 1b) [34]. In both techniques, the interaction between the target and the recognition element (i.e. aptamer) can sensitively be monitored. Examples of biosensor applications of SE and SPR-TIRE techniques can be found in the literature [34–36]. So far, to the best of our

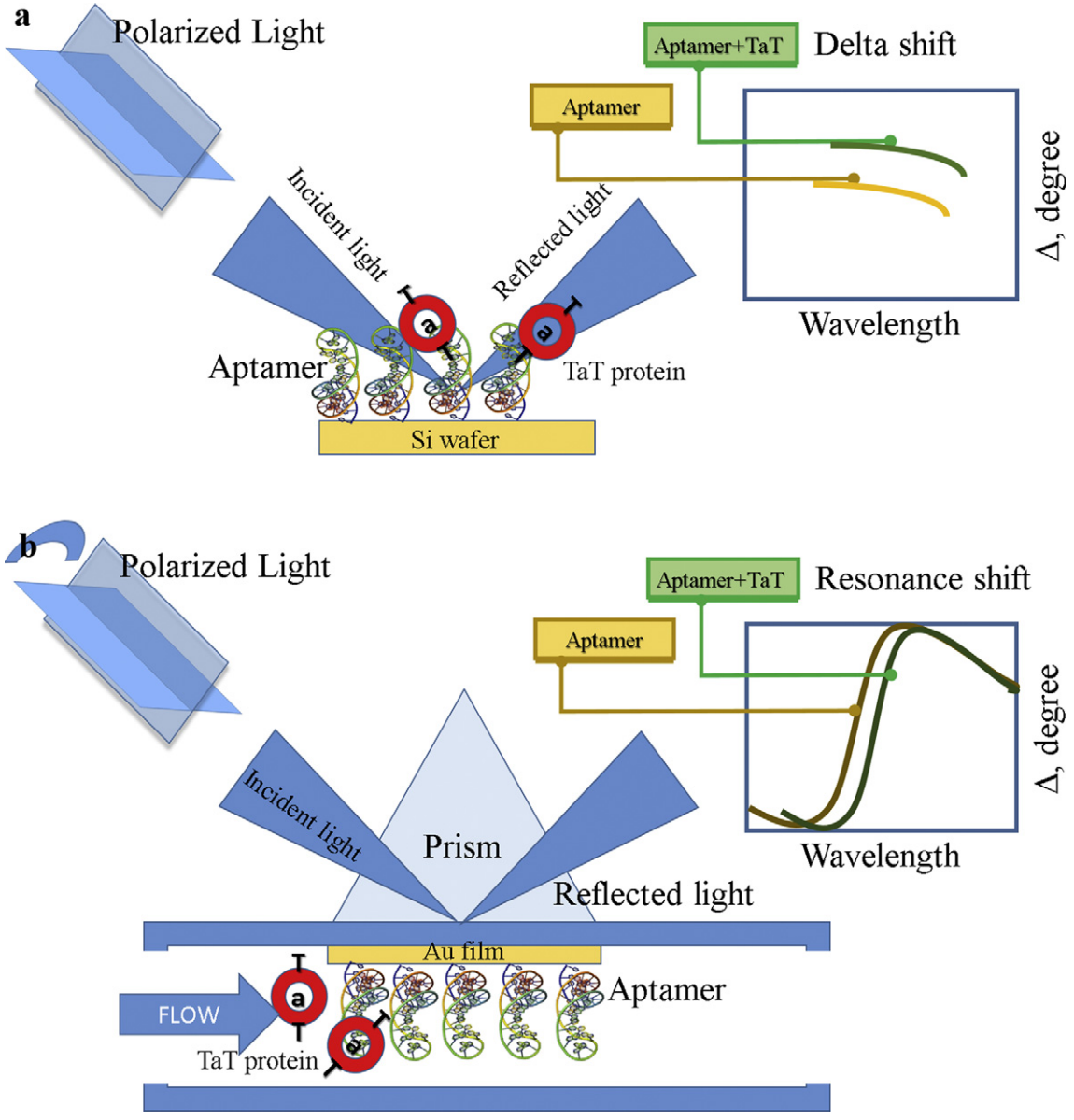

Fig. 1. Schematic drawing of a) SE setup and its usual sensor response; b) SPReTIRE setup and its usual sensor response.

Table 1
antiTat aptamers used in this study.

Aptamer	Array
AntiTat1	5′-SH-$(CH_2)_6$-ACGA AGCU UGAU CCCG UUUG CCGG UCGA UCGC UUCGA-3′
AntiTat2	5′-SH-$(CH_2)_6$-$(A)_{10}$-ACGA AGCU UGAU CCCG UUUG CCGG UCGA UCGC UUCGA-3′
AntiTat3	5′-NH_2-$(CH_2)_6$-ACGA AGCU UGAU CCCG UUUG CCGG UCGA UCGC UUCGA-3′
AntiTat4	5′-NH_2-$(CH_2)_6$-$(A)_{10}$-ACGA AGCU UGAU CCCG UUUG CCGG UCGA UCGC UUCGA-3′
AntiTat5 (hair-pin type)	5′-NH_2-$(CH_2)_6$-**ACGA AGCU UGAU CCCG UUUG CCGG UCGA UCGC UUCG A**AAA AAAA AAAA CGAA GCUU GAUC CCGU UUGC CGGU CGAU CGCU UCG-3′

knowledge, there is no published study in the literature on the sensitive detection of HIV-related proteins by ellipsometry, spectroscopic ellipsometry or total internal reflection ellipsometry.

2. Materials and methods

2.1. Optimization of anti-Tat aptamer immobilization conditions on Au and Si surface

Anti-Tat aptamers, which are thiol and amine-functionalized at 5′ end, were immobilized on two different platforms. Aptamers used in this study are listed in Table 1.

All containers to be used during the experiment were cleaned with a blocking solution (RNaseZAP) to prevent RNA degradation via ribonuclease. Sensor chips (50 nm Au film coated BK7 type glass slides or Si wafer pieces) were immersed in the oxidative solution consisting of a mixture of H_2SO_4 and H_2O_2 (v/v 7:3) for 2 s, and then rinsed well with ethyl alcohol. The metal film was physically coated on a pre-cleaned and plasma-treated glass slides using physical vapor deposition method. The coating thickness was 50 nm Au as over-layer coating of 3 nm Cr. Following this process, the sensor chips (Au-chips) were re-cleaned under plasma (100 W/ air) in a Diener (Germany) model plasma device.

AntiTat1 and AntiTat2 aptamers prepared (1.0–1.0 μM) in HEPES buffer (0.01 M N-2-hydroxyethyl piperazine-N′-2-ethanesulfonic acid, 0.15 M NaCl, 3 mM EDTA and 0.005% polyoxyethylene sorbitomonolaurate) were immobilized on the Au-chips under SPRe-TIRE conditions. Then, Au-chip surface was blocked using 6-mercapto-1-hexanol (MCH) to minimize non-specific interactions. The thickness of the layer on the sensor chips was monitored via ellipsometric measurements at each stage. The surface roughness was also determined by atomic force microscopy.

AntiTat3, AntiTat4, and AntiTat5 aptamers were immobilized on the modified silicon (Si) wafer (Si-chips). Si wafers cut into 1 cm × 1 cm were wet cleaned with nitric acid, hydrogen peroxide and ethyl alcohol, acetone, and water after the plasma treatment for 30 min. Then, the mercaptopropyl triethoxysilane (MPTES), prepared in absolute ethyl alcohol was used for -SH functionalization. Immobilization on the surface was monitored by ellipsometric thickness measurement. Mercapto undecanoic acid (MUA) was used for —COOH functionalization on Si-chips. NH_2-functionalized aptamers were then immobilized on the —COOH functionalized over-layer via 1-ethyl-3-(3-dimethylaminopropyl) carbodiimide (EDAC) route. In this step, where concentration and exposure times have been optimized, the thickness of the organic layer deposited on the Si-chips was confirmed using an ellipsometer.

2.2. Determination of the sensor performance

The HIV-1 Tat protein detection performances of the AntiTat3–AntiTat5 assays were determined using HIV-Tat solutions (1.0–500 nM) prepared in the buffer solution. Si-chips were washed with buffer solution (HEPES) after dipping into the HIV-Tat solution. Si-chips were then analyzed using spectroscopic ellipsometer to obtain the delta (Δ) and psi (Ψ) for 200–1200 nm. The sensor response was evaluated as Δ and ψ variations. The Δ angle (in other words, the phase shift between polarization states) was selected as sensor response since it was more sensitive to the surface deposition (the thickness and refractive index changes).

The analytical performances of the AntiTat1 and AntiTat2 aptamer assays were evaluated using SPRe-TIRE. For this purpose, Au-chips were washed using HEPES in a flow cell consisting of a BK7 glass prism (R.I. 1.58) to get a baseline signal. The HIV-Tat solutions in different concentrations (1.0–500 nM) were then analyzed using delta (Δ) and psi (Ψ) measurements. First, spectrum was scanned between 200 nm and 1200 nm to find the SPR wavelength where Δ has an infinite slope. Then the amount of protein captured by the aptamer was evaluated as Δ changes.

Sensor calibration graphs were plotted as Δ vs HIV-Tat concentration, then the detection sensitivity and the detection limit (LOD) were calculated. Bovine serum albumin (BSA) was used for the specificity analysis.

2.3. Thickness measurements and roughness analysis

The thickness of accumulated molecule layer on each chip surface was measured then calculated using both Δ and Ψ via built in model-solver of the equipment. All thickness measurements were done on the 3 test specimen, for at least 10 random measurement points. Surface topography images of the samples were obtained using a ParkSystems XE-100 model atomic force microscopy (AFM) equipment (Suwon, Korea) to carry out a roughness analysis using built-in software of the equipment. 512 × 512-pixel topography images were acquired in air using CM-silicon probes (Park Systems, Korea) in contact mode. Roughness analyses were carried out on 4 test specimens at minimum 10 randomly selected points.

3. Results and discussions

3.1. Optimization of anti-aptamer immobilization conditions on Si and Au surface

In Table 2, ellipsometric thickness data for definite time intervals of immobilization are given. Ellipsometric thickness was calculated using equipment built-in software by modeling, according to model parameters for BK7 substrate/Cr layer/Au layer/Organic layer ($n = 1.46$)/Air multilayer model.

The thickness of the accumulated organic layer was steady at around 300 s. The RMS roughness obtained from the topography analysis also increased with the immobilization duration. Moreover, the longer immobilization durations also resulted in surface non-uniformity as obtained from standard deviation value. RMS roughness for bare Au-coated material was 0.89 ± 0.11 nm. It was decided that 2 min buffer flow after 5 min AntiTat1 (1.00 μM) circulation were appropriate for

Table 2
Thicknesses for 0.1 μM AntiTat1 immobilization.[a]

Time (s)	Thickness (nm)	RMS roughness (nm)
s	0.68 ± 0.09	1.46 ± 0.08
120	0.97 ± 0.11	1.35 ± 0.12
240	1.12 ± 0.14	1.88 ± 0.11
300	1.89 ± 0.12	2.81 ± 0.31
1500	1.96 ± 0.10	2.94 ± 0.61

[a] The number of repetitions is 3.

Table 3
Optimum parameters for probe immobilization on Au surface.

Aptamer	Time (s)	Probe concentration	Sensor signal at the optimum conditions (Δ, degree)
AntiTat1	300	1.00 μM	4.18 ± 0.11
AntiTat2	300	1.00 μM	4.51 ± 0.24

the immobilization. Immobilization parameters for other aptamer probes are given in Table 3.

AntiTat3 to AntiTat5 aptamers were immobilized on the modified Si wafer to obtain an assay method that can easily evolve into microfluidic channels on glass slides suitable for the "lab on a chip" applications. Two mechanisms are effective in the formation of self-assembled monolayers. These mechanisms, in turn, are surface adsorption and covalent bonding. Both steps depend on the concentration of the silanol and the duration of the interaction of the molecules at certain concentrations with the surface. The thickness variations of Si-wafer immersed in 1 μM MPTES solution were determined as 0.46 ± 0.03, 0.93 ± 0.02, 0.98 ± 0.02, 1.63 ± 0.02 and 2.21 ± 0.03 nm for 1, 2, 3, 4 and 8 h, respectively. Thicknesses were determined by ellipsometric measurements where Si/SiO_2 oxide layer/organic layer (Cauchy model)/air materials were selected from the equipment library as model parameters. In the first 3 h, a formation thickness corresponding to the single-layer deposition was observed on the surface. Beyond 3 h, an increase in thickness indicated the formation of macromolecules on the surface. The increase in thickness for long periods was probably as a result of the accumulation of MPTES-mers on the surface due to the air moisture, which is not avoidable unless using an air-conditioned environment. For this reason, the optimum immobilization duration was selected as 2 h (in the dark, at the room temperature). The effect of MPTES concentration on monolayer formation (50, 10, 5, 1 and 0.5 μM MPTES/absolute ethyl alcohol solution) was investigated. Thicknesses at 0.5 and 1.0 μM were determined as 1.09 ± 0.027 nm and 1.31 ± 0.021 nm, respectively. Thus, MPTES at a concentration of 1.0 μM was found to be suitable for the formation of the desired layer. Subsequent surface modification with MUA was performed to achieve carboxyl terminated functional surface. The disulfide reaction was carried out for 2, 4, 8, 12 and 24 h (Table 4) with 1.0 μm MUA at room temperature, in the dark, in a vacuum and a nitrogen-swept closed container. The optimum layer-formation conditions for MUA/MPTES interaction were selected as 8 h for 5 μM MUA, according to the thickness measurements. The optimum parameters for AntiTat3 to AntiTat5 binding via EDAC route were 1.5 μM aptamer and 2 h.

3.2. SE and SPRe-TIRE sensor performance

The interaction between the AntiTat assay and the Tat protein (1 nM to 500 nM in the buffer) was evaluated between 400 nm and 1700 nm by SE. The Δ-λ relation between 600 and 700 nm was almost-linear with the 0.94 regression coefficient (R^2), since the material deposited on the surface is an organic layer. This linear-relation zone shifted to the lower Δ values due to the antiTat-Tat interactions. This shift (Δ) was selected as sensor response and the calibration curve was plotted.

Table 4
Ellipsometric thickness and roughness measurements for MUA monolayer formation.[a]

Time (hours)	Thickness (nm, as over layer)	RMS roughness (nm)
2	0.84 ± 0.32	7.72 ± 1.94
4	0.95 ± 0.21	8.90 ± 1.21
8	1.23 ± 0.18	8.12 ± 1.89
12	1.38 ± 0.17	9.02 ± 0.76
24	1.27 ± 0.17	8.88 ± 1.02

[a] The number of repetitions is 3.

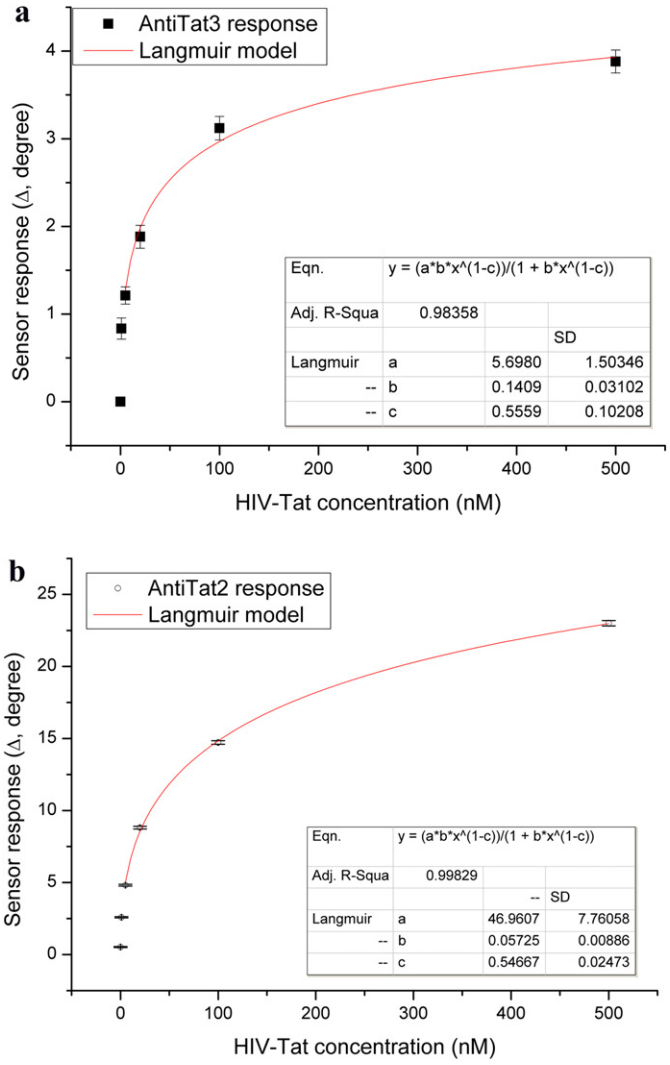

Fig. 2. Sensor calibration curves for (a) AntiTat3 aptamer (SE configuration) and (b) AntiTat2 aptamer (SPRe-TIRE configuration), under optimized conditions.

The calibration curve obtained for the AntiTat3 and its fitting results (for the Langmuir model) is given in Fig. 2a.

The interaction between the aptamer on the sensor surface and the captured HIV-Tat protein took place in a single site, and the binding rate decreased with the amount of the free aptamer. The aptamer

Table 5
Sensor performance for SE and SPRe-TIRE.[a]

Aptamer	Platform	Coefficients of Langmuir model	Regression coefficient, R^2	LOD (3σ)
AntiTat3	SE	a = 5.6980 b = 0.1409 c = 0.5559	0.98	194 pM
AntiTat4	SE	a = 7.8581 b = 0.0936 c = 0.5067	0.95	151 pM
AntiTat5	SE	a = 8.6201 b = 0.0396 c = 0.1342	0.98	1.88 nM
AntiTat1	SPRe-TIRE	a = 24.5674 b = 0.0841 c = 0.4794	0.99	17.9 pM
AntiTat2	SPRe-TIRE	a = 46.961 b = 0.0573 c = 0.5467	0.99	1.11 pM

[a] The number of repetitions is 3, 1.0–500 nM active range.

Table 6
Comparison of HIV detection methods.

Method	Element	Active/Linear range	LOD	Methodology	References
Electrochemical cyclic voltammetry (CV)	HIV-gp120 antibody	600 fg/mL–375 pg/mL	NR	Direct measurement of HIV virus like particles (VLPs), direct electron transfer based on CV, without mediators	[37]
Surface plasmon resonance (SPR) and localized SPR	HIV-gp120 antibody	200 fg/mL–125 pg/mL	200 fg/mL	Direct measurements of VLPs on Au-dots fabricated on ITO coated glass substrate	[38]
Electrochemical CV	HIV-NF-κB protein specific aptamer sequence	5–500 nM	7.05 pM	Sandwich like aptasensor, NF-κB protein, HRP and H_2O_2 mediated oxidation	[39]
Electrochemical	HIV oligonucleotide (ON) sequence complementary ON probe	20–100 nM	0.1 nM	Hair-pin, HIV specific ON probes immobilized on multi electrode array, square wave voltammetry	[40]
Nanomechanical (Piezocrystal)	HIV-gp24 antibody	NR	10^{-17} g/mL	Sandwich immunoassay combines nanomechanical and optoplasmonic methods, antibody (Ab) immobilized microcantilever and Ab immobilized AuNPs	[41]
Nanomechanical	HIV-gp24 antibody	17–1680 $TCID_{50}$ (tissue culture infective dose 50%)	12 $TCID_{50}$ (approx. 3400 viral particles eq.)	Sandwich immunoassay nanomechanical methods	[42]
Scanning tunneling microscopy (STM)	HIV-gp120 antibody	200 fg/mL–125 pg/mL VLPs	200 fg/mL HIV-VLPs	Direct detection of HIV-VLPs by using AuNPs	[43]
Electrochemical differential pulse voltammetry (DPV)	HIV-gp24 antibody	0.001–10 ng/mL	0.5 pg/mL	Sandwich type immunoanalysis with SiO_2 coated Fe_3O_4 nanoparticles conjugated with gp24 antibody and signal tag AuNPs/EnVision reagent	[44]
Electrochemical impedance spectroscopy (EIS)	HIV-gp24 antibody	0.01–60 ng/mL	6.4 pg/mL	AuNP/multi-walled carbon nanotube (MWCNTs)/acetone-extracted propolis nanocomposite	[45]
Electrochemical CV	HIV-gp160 antibody	1–400 ng/mL	0.5 ng/mL	Fe_3O_4/Au core-shell particle and chitosan nanocomposite film on glassy carbon electrode, copper complex as electron transfer mediator	[46]
Electrochemical CV and DPV	HIV-gp24 antibody	0.6–160 μg/mL	0.32 ng/mL	Fe_3O_4/Au core-shell particle/MW-CNTs composite on screen printed electrode	[47]
Diffraction	HIV-gp120 antibody	10^4 copies/mL−10^8 copies/mL	NR	TiO_2 surface with silanol, succinimide ester and NeutrAvidin modification	[48]
Spectroscopic ellipsometry	antiTat protein aptamer	1.0–500 nM	151 pM	Direct measurement of phase shit on aptamer immobilized Si surface	This work
SPRe-TIRE	antiTat protein aptamer	1.0–500 nM	1.11 pM	Signal amplification via SPR on SE system	This work

AntiTat4 and AntiTat3 carrying A_{10} as spacer unit did not show a significant difference in terms of affinity (c coefficient in Table 5). Model parameters of AntiTat5 probe (hairpin type) were smaller than other probes. While the LOD for AntiTat3 and AntiTat4 probes were around 200 pM, the LOD for AntiTat5 was 10 times higher than the others. Sensor responses of both aptamers (i.e. linear and hairpin type) were highly satisfactory in terms of LODs and comparable with the conventional ELISA methods (with a detection limit of 0.29 pg/mL–2.9 ng/mL). To determine analytical performances of Au-chip assays 0 nM −500 nM Tat solution was injected into the SPRe-TIRE flow cell. The flow rate was 5 μL/min and the reaction was carried out at room temperature. The calibration graph for SPRe-TIRE is shown in Fig. 2b. As expected, the interaction between the aptamer and the protein fits well to the single-site binding like the Langmuir model. Coefficients of the Langmuir model and sensor detection limits are given in Table 5.

In the closed-loop system such as SPRe-TIRE flow cell where additional steps such as washing and drying outside of the cell were not necessary, higher regression coefficients for calibration curve fitting parameters were obtained. Furthermore, in the SPRe-TIRE configuration, the detection limit was lower (1 pM or 1.5 pg/mL) than the SE configuration due to signal amplification at SPR conditions.

3.3. The specificity of SE and SPRe-TIRE sensors

To check the specificity, 100 nM BSA was added in the sample solution at specified conditions. The sensor response was also checked by sending 100 nM HIV-1 Tat followed by only 100 nM BSA. The BSA sent at a median concentration (100 nM) relative to the sensor operating range caused a signal increase of less than 10% of the original response. In the case, where only BSA was added, the sensor response (0.252°) was smaller than the LOD.

3.4. The other HIV-specific methods

Some of the electrochemical, optical, nanomechanical and scanning probe techniques for the detection of HIV/HIV-related proteins/HIV specific oligonucleotides are listed in Table 6. Most of these studies listed are immunoassays based on HIV glycol-proteins such as gp24 and gp120. Moreover, ranges and detection limits of these studies are within the range of pg/mL to ng/mL and there are no significant differences between them, in terms of analytical performances. Although the listed methods are easy, reliable and comparable with ELISAs, our suggested method has another advantage of using aptamers which are quite stable than the protein-based assays.

4. Conclusion

Ellipsometry-based sensors have been developed for HIV diagnosis, using 5 kinds of HIV-Tat aptamers that have the same specific functional sequence but have different surface immobilization pathways. These sensors have been successfully used in determining the Tat protein over a range of 1 nM −500 nM, in the buffer solution. The SPRe-TIRE configuration using the AntiTat2 probe revealed a minimum detection limit of 1 pM (or about 1.5 pg/mL), The detection mechanism for all sensor configurations proposed was single site interaction which was confirmed by high correlation coefficients for the Langmuir model.

Acknowledgments

The author is grateful to the Cumhuriyet University, Scientific Research Projects Support Department (CUBAP) for the financial support under grant number M584.

Declaration of competing interest

The authors declare that they have no known competing financial interests or personal relationships that could have appeared to influence the work reported in this paper.

References

[1] S.A. Schwartz, M.P.N. Nair, Current concepts in human immunodeficiency, Clin. Diagn. Lab. Immunol. 6 (1999) 295–305.
[2] J.W. Mellors, C.R. Rinaldo Jr., P. Gupta, R.M. White, J.A. Todd, L.A. Kingsley, Prognosis in HIV-1 infection predicted by the quantity of virus in plasma, Science 272 (1996) 1167–1170.
[3] G. Pantaleo, C. Graziosi, A.S. Fauci, Virologic and immunologic events in primary HIV infection, Springer Semin. Immunopathol. 18 (1997) 257–266.
[4] C. Sood, M. Marin, C.S. Mason, G.B. Melikyan, Visualization of content release from cell surface-attached single HIV-1 particles carrying an extra-viral fluorescent pH-sensor, PLoS One 11 (2016), e0148944.
[5] A. Biancotto, B. Brichacek, S.S. Chen, W. Fitzgerald, A. Lisco, C. Vanpouille, L. Margolis, J.C. Grivel, A highly sensitive and dynamic immunofluorescent cytometric bead assay for the detection of HIV-1 p24, J. Virol. Methods 157 (2009) 98–101.
[6] S.A. Fiscus, C.D. Pilcher, W.C. Miller, K.A. Powers, I.F. Hoffman, M. Price, D.A. Chilongozi, C. Mapanje, R. Krysiak, S. Gama, F.E. Martinson, M.S. Cohen, Rapid, real-time detection of acute HIV infection in patients in Africa, J. Infect. Dis. 195 (2007) 416–424.
[7] R.A. Respess, A. Cachafeiro, D. Withum, S.A. Fiscus, D. Newman, B. Branson, O.E. Varnier, K. Lewis, T.J. Dondero, Evaluation of an ultrasensitive p24 antigen assay as a potential alternative to human immunodeficiency virus type 1 RNA viral load assay in resource-limited settings, J. Clin. Microbiol. 43 (2005) 506–508.
[8] R. Sutthent, N. Gaudart, K. Chokpaibulkit, N. Tanliang, C. Kanoksinsombath, P. Chaisilwatana, p24 Antigen detection assay modified with a booster step for diagnosis and monitoring of human immunodeficiency virus type 1 infection, J. Clin. Microbiol. 41 (2003) 1016–1022.
[9] V. Black, C.E. von Mollendorf, J.A. Moyes, L.E. Scott, A. Puren, W.S. Stevens, Poor sensitivity of field rapid HIV testing: implications for mother-to-child transmission programme, BJOG Int. J. Obstet. Gynaecol. 116 (2009) 1805–1808.
[10] T.M. Gronewold, Surface acoustic wave sensors in the bioanalytical field: recent trends and challenges, Anal. Chim. Acta 603 (2007) 119–128.
[11] A. Niemz, T.M. Ferguson, D.S. Boyle, Point-of-care nucleic acid testing for infectious diseases, Trends Biotechnol. 29 (2011) 240–250.
[12] M.K. Haleyur Giri Setty, I.K. Hewlett, Point of care technologies for HIV, AIDS Res Treat 2014 (2014), 497046.
[13] M.B. Wabuyele, T. Vo-Dinh, Detection of human immunodeficiency virus type 1 DNA sequence using plasmonics nanoprobes, Anal. Chem. 77 (2005) 7810–7815.
[14] N. Thelwell, S. Millington, A. Solinas, J. Booth, T. Brown, Mode of action and application of scorpion primers to mutation detection, Nucleic Acids Res. 28 (2000) 3752–3761.
[15] M.J.A. Shiddiky, A.A.J. Torriero, Z. Zeng, L. Spiccia, A.M. Bond, Highly selective and sensitive DNA assay based on electrocatalytic oxidation of Ferrocene bearing zinc (II)−Cyclen complexes with diethylamine, J. Am. Chem. Soc. 132 (2010) 10053–10063.
[16] K.M. You, S.H. Lee, A. Im, S.B. Lee, Aptamers as functional nucleic acids:in vitro selection and biotechnological applications, Biotechnol. Bioprocess Eng. 8 (2003) 64–75.
[17] E. Luzi, M. Minunni, S. Tombelli, M. Mascini, New trends in affinity sensing, TrAC Trends Anal. Chem. 22 (2003) 810–818.
[18] C. Tuerk, L. Gold, Systematic evolution of ligands by exponential enrichment: RNA ligands to bacteriophage T4 DNA polymerase, Science 249 (1990) 505–510.
[19] A.D. Ellington, J.W. Szostak, In vitro selection of RNA molecules that bind specific ligands, Nature 346 (1990) 818–822.
[20] K.A. Marshall, A.D. Ellington, In vitro selection of RNA aptamers, Methods Enzymol. 318 (2000) 193–214.
[21] R.D. Jenison, S.C. Gill, A. Pardi, B. Polisky, High-resolution molecular discrimination by RNA, Science 263 (1994) 1425–1429.
[22] S. Tombelli, M. Minunni, M. Mascini, Analytical applications of aptamers, Biosens. Bioelectron. 20 (2005) 2424–2434.
[23] Y. Zhang, B.S. Lai, M. Juhas, Recent advances in Aptamer discovery and applications, Molecules 24 (2019) 941.
[24] Z. Zhuo, Y. Yu, M. Wang, J. Li, Z. Zhang, J. Liu, X. Wu, A. Lu, G. Zhang, B. Zhang, Recent advances in SELEX technology and Aptamer applications in biomedicine, Int. J. Mol. Sci. 18 (2017) 2142.
[25] X. Zou, J. Wu, J. Gu, L. Shen, L. Mao, Application of Aptamers in virus detection and antiviral therapy, Front. Microbiol. 10 (2019).
[26] H.C. Chang, F. Samaniego, B.C. Nair, L. Buonaguro, B. Ensoli, HIV-1 tat protein exits from cells via a leaderless secretory pathway and binds to extracellular matrix-associated heparan sulfate proteoglycans through its basic region, AIDS (London, England) 11 (1997) 1421–1431.
[27] P. Mucha, A. Szyk, P. Rekowski, J. Barciszewski, Structural requirements for conserved Arg52 residue for interaction of the human immunodeficiency virus type 1 trans-activation responsive element with trans-activator of transcription protein (49-57). Capillary electrophoresis mobility shift assay, J. Chromatogr. A 968 (2002) 211–220.
[28] I. D'Orso, A.D. Frankel, HIV-1 Tat: its dependence on host factors is crystal clear, Viruses 2 (2010) 2226–2234.
[29] V. Penmatsa, R.A. Rahim, H. Kawarada, C. Wang, Functionalized carbon microarrays platform for high sensitive detection of HIV-Tat peptide, RSC Adv. 5 (2015) 65042–65047.
[30] Y. Rao, S.J.J. Kwok, J. Lombardi, N.J. Turro, K.B. Eisenthal, Label-free probe of HIV-1 TAT peptide binding to mimetic membranes, Proc. Natl. Acad. Sci. 111 (2014) 12684–12688.
[31] R. Yamamoto, M. Katahira, S. Nishikawa, T. Baba, K. Taira, P.K. Kumar, A novel RNA motif that binds efficiently and specifically to the Ttat protein of HIV and inhibits the trans-activation by Tat of transcription in vitro and in vivo, Genes to cells: devoted to molecular & cellular mechanisms 5 (2000) 371–388.
[32] M. Minunni, S. Tombelli, A. Gullotto, E. Luzi, M. Mascini, Development of biosensors with aptamers as bio-recognition element: the case of HIV-1 Tat protein, Biosens. Bioelectron. 20 (2004) 1149–1156.
[33] G.E. Jellison, 3 Data analysis for spectroscopic Ellipsometry, in: H.G. Tompkins, E.A. Irene (Eds.), Handbook of Ellipsometry, William Andrew Publishing, Norwich, NY 2005, pp. 237–296.
[34] M.O. Çağlayan, F. Sayar, G. Demirel, B. Garipcan, B. Otman, B. Çelen, E. Pişkin, Stepwise formation approach to improve ellipsometric biosensor response, Nanomedicine 5 (2009) 152–161.
[35] A. Keske, A. Atar, İ. Üstündağ, M.O. çağlayan, Detection of influenza A by surface plasmon resonance enhanced Total internal reflection ellipsometry, J. Comput. Theor. Nanosci. 11 (2014) 981–986.
[36] Z. Ustundag, M.O. Caglayan, R. Guzel, E. Piskin, A.O. Solak, A novel surface plasmon resonance enhanced total internal reflection ellipsometric application: electrochemically grafted isophthalic acid nanofilm on gold surface, Analyst 136 (2011) 1464–1471.
[37] J.-H. Lee, B.-K. Oh, J.-W. Choi, Electrochemical sensor based on direct electron transfer of HIV-1 virus at au nanoparticle modified ITO electrode, Biosens. Bioelectron. 49 (2013) 531–535.
[38] J.H. Lee, B.C. Kim, B.K. Oh, J.W. Choi, Highly sensitive localized surface plasmon resonance immunosensor for label-free detection of HIV-1, Nanomedicine 9 (2013) 1018–1026.
[39] Y. Guo, J. Chen, G. Chen, A label-free electrochemical biosensor for detection of HIV related gene based on interaction between DNA and protein, Sensors Actuators B Chem. 184 (2013) 113–117.
[40] D. Zhang, Y. Peng, H. Qi, Q. Gao, C. Zhang, Label-free electrochemical DNA biosensor array for simultaneous detection of the HIV-1 and HIV-2 oligonucleotides incorporating different hairpin-DNA probes and redox indicator, Biosens. Bioelectron. 25 (2010) 1088–1094.
[41] P.M. Kosaka, V. Pini, M. Calleja, J. Tamayo, Ultrasensitive detection of HIV-1 p24 antigen by a hybrid nanomechanical-optoplasmonic platform with potential for detecting HIV-1 at first week after infection, PLoS One 12 (2017), e0171899.
[42] M. Bisoffi, V. Severns, D.W. Branch, T.L. Edwards, R.S. Larson, Rapid detection of human immunodeficiency virus types 1 and 2 by use of an improved piezoelectric biosensor, J. Clin. Microbiol. 51 (2013) 1685–1691.
[43] J.-H. Lee, B.-C. Kim, B.-K. Oh, J.-W. Choi, Highly sensitive electrical detection of HIV-1 virus based on scanning tunneling microscopy, J. Nanosci. Nanotechnol. 15 (2015) 1117–1122.
[44] N. Gan, X. Du, Y. Cao, F. Hu, T. Li, Q. Jiang, An ultrasensitive electrochemical Immunosensor for HIV p24 based on Fe_3O_4@SiO_2 nanomagnetic probes and nanogold colloid-labeled enzyme–antibody copolymer as signal tag, Materials 6 (2013) 1255.
[45] F. Kheiri, R.E. Sabzi, E. Jannatdoust, E. Shojaeefar, H. Sedghi, A novel amperometric immunosensor based on acetone-extracted propolis for the detection of the HIV-1 p24 antigen, Biosens. Bioelectron. 26 (2011) 4457–4463.
[46] N. Gan, L.-Y. Wang, T.-H. Li, L. Zheng, F. Wang, Reagentless amperometric immunosensor based on human immunodeficiency virus diagnosis marker glycoprotein 160 antibody coated Gold-magnetic particles modified electrode, Chin. J. Anal. Chem. 37 (2009) 1125–1130.
[47] N. Gan, N.-X. Luo, T.-H. Li, L. Zheng, M.-J. Ni, A non-enzyme amperometric immunosensor for rapid determination of human immunodeficiency virus p24 based on magnetism controlled carbon nanotubes modified printed electrode, Chin. J. Anal. Chem. 38 (2010) 1556–1562.
[48] H. Shafiee, E.A. Lidstone, M. Jahangir, F. Inci, E. Hanhauser, T.J. Henrich, D.R. Kuritzkes, B.T. Cunningham, U. Demirci, Nanostructured optical photonic crystal biosensor for HIV viral load measurement, Sci. Rep. 4 (2014) 4116.